J Appl Electrochem (2010) 40:1511–1517
DOI 10.1007/s10800-010-0129-3

ORIGINAL PAPER

Electrocoagulation of fermentation wastewater by low carbon steel (Fe) and 5005 aluminium (Al) electrodes

Andrew Gadd · Dan Ryan · John Kavanagh · Anne-Laure Beaurain · Simon Luxem · Geoff Barton

Received: 9 August 2009 / Accepted: 27 March 2010 / Published online: 11 April 2010

Abstract Successful application of electrocoagulation technology requires a thorough evaluation of electrode behaviour. This study is concerned with the treatment of fermentation wastewater, generated by molasses-fed biorefineries in large volumes and containing high concentrations of biorecalcitrant, coloured organic melanoidins that form a highly dispersed colloid. The polarisation behaviour, surface morphology and current efficiency of both hot rolled coil steel and 5005 aluminium electrodes were investigated. The steel electrodes were found to be susceptible to aggressive anodic pitting which is attributed to the high chloride content of the wastewater, while the aluminium exhibited anomalous corrosion of the anode and cathode. The redox potential of the wastewater has a significant effect on Fe^{2+}/Fe^{3+} speciation with steel electrodes and thus on the decolourising efficiency of electrocoagulation. The practical implications of the corrosion characteristics are discussed.

Keywords Electrocoagulation · Current efficiency · Cyclic voltammetry · Iron speciation · Fermentation wastewater

1 Introduction

Electrocoagulation (EC), also referred to as electroflocculation, is an attractive alternative to conventional tertiary water treatment technologies for a broad range of challenging industrial wastewaters. It has been successfully applied to a wide range of effluents including electroplating processes, tanneries, chipset manufacture, textile dyes, oil/water emulsions and many others [1]. Its wide applicability arises from the fact that the metal species generated interact with both inorganic and organic pollutants over a wide size range. When appropriately designed and operated, EC is flexible, compact, energy efficient and cost effective [2].

EC is a particularly attractive treatment option for high-strength biorecalcitrant organic colloids where conventional treatments are impractical and/or uneconomic. This study is part of a wider investigation into the application of EC to fermentation wastewater. This wastewater is generated during the production of ethanol and food products by fermentation of cane molasses. Globally, fuel ethanol production from fermentation is expected to reach 50 GL $year^{-1}$ in 2010. A substantial barrier to the sustainability of this rapidly expanding industry is the management and treatment of the wastewater streams, as for each litre of ethanol produced, typically 6–20 L of fermentation wastewater are generated [3].

Secondary treatment of this fermentation wastewater removes the bulk of the organic load but a heavy loading of intensely coloured melanoidins remains as a stable colloid. Further treatment by oxidation technologies is generally effective on the colour but not COD [4, 5], filtration processes are prone to fouling [6], and reverse osmosis generates a high salinity retentate that presents disposal difficulties [7]. Chemical coagulation removes colour and COD relatively effectively, but has a number of drawbacks [8]. The advantages of EC compared to conventional chemical coagulation include reduced wastewater acidification and salinity, superior coagulant dispersion and intrinsic electroflotation separation capability [9].

A. Gadd (✉) · D. Ryan · J. Kavanagh · A.-L. Beaurain · S. Luxem · G. Barton
School of Chemical and Biomolecular Engineering, University of Sydney, Sydney, NSW 2006, Australia
e-mail: a.gadd@usyd.edu.au

Initial investigations established that continuous EC with either steel or aluminium electrodes could remove up to 99% of the visible colour (UV_{475}) and 80% of the COD from fermentation wastewater, which is comparable to chemical coagulation with either aluminium sulfate or ferric chloride [10]. Here a current density (j) range of 1–5 mA cm^{-2} was used, as this would provide a reasonable compromise between hydraulic loading (reactor size) and electrode life for a full-scale EC reactor.

The operational efficiency of EC treatment is largely determined by the consumption of power and metal required to generate the coagulant. Characterising the electrode behaviour enables operating efficiency improvement, while predictable corrosion behaviour simplifies process control. Closer examination of the electrode interface was therefore deemed an essential element in this industrially sponsored research prior to any commercial application.

1.1 Electrochemistry at the electrode interface

An EC reactor is an electrolytic cell comprising metal electrodes with the wastewater acting as the cell electrolyte. Metal ions are generated by oxidation at the anode surface with the general reaction being:

$$Me_{(s)} \rightarrow Me^{z+} + ze^{-} \quad (1)$$

The metal ions rapidly hydrolyse to form a range of active coagulant ligands as they diffuse into the bulk solution. Simultaneously, cathodic reduction takes place to satisfy charge conservation producing hydrogen under neutral or alkaline conditions via:

$$2H_2O_{(l)} + 2e^{-} \rightarrow 2OH^{-} + H_{2(g)} \quad (2)$$

as well as under acidic conditions via:

$$2H^{+} + 2e^{-} \rightarrow H_{2(g)} \quad (3)$$

Ideally all the anodic current is consumed by Eq. 1, where Faraday's Law can be used to predict the dissolution rate:

$$m = \frac{ItM}{zF} \quad (4)$$

where m = mass of metal dissolved (g), I = current (A), t = time (s), M = molecular weight of the electrode metal (g mol^{-1}), z = oxidation state of the dissolved metal, and F = Faraday constant (96 485 C mol^{-1}). The actual dissolution rate, however, may deviate significantly from this relationship due to a range of nonfaradaic processes [11–15]. Current efficiency (ϕ) is an experimentally determined correction factor that accounts for anomalous dissolution of the electrodes. Introducing ϕ and rearranging Eq. 4 gives:

$$Y_{Me} = a\frac{j\phi M}{zF} \quad (5)$$

where Y_{Me} = actual space-time yield of metal (g m^{-3} h^{-1}), a = specific electrode area (m^2 m^{-3}), and j = current density (A m^{-2}).

1.2 Oxidation state of iron in EC

For iron electrodes, there is disagreement in the literature regarding the anodic oxidation occurring in an EC reactor. The electrolytic oxidation of iron is predominantly ferrous (z = 2) [1, 16]. However in some electrolytes, ferric (z = 3) corrosion has been shown to dominate, for example where a significant level of chloride is present [17, 18]. Further electrolytic oxidation to ferrate (z = 6) has also been demonstrated and is an area of ongoing research [19, 20], as ferrate species are very effective coagulants.

Solution conditions near an electrode surface can be quite different to those in the bulk solution. As a result of the rapid hydrolysis of metal dissociating from the surface, the anodic interfacial layer is acidic. The redox potential is also high due to the polarised state of the anode, which favours higher oxidation states. The valency of metal corroded at the anode and the speciation in the bulk solution are critical influences in the overall efficiency of the EC process.

The objective of this work was thus to clarify the rationale underpinning the choice of electrode material (i.e. iron or aluminium) and reactor conditions for the treatment of fermentation wastewater by EC. This was achieved as follows: (i) by analysing the corrosion behaviour of aluminium and mild steel electrodes in fermentation wastewater using cyclic voltammetry, (ii) by examining the surface morphology of the electrodes after polarisation, and (iii) by determining the current efficiency of the system under a range of operational conditions appropriate for a full-scale EC reactor.

2 Experimental methodology

2.1 Materials

Electrode materials must be low-cost and readily available to be practical for use in industrial-scale EC. Accordingly, low carbon hot rolled coil (HRC) steel (AS/NZS 1594:HA1) and 5005 aluminium (>97% Al) were selected. Fermentation wastewater was collected from a yeast production facility after it had undergone full secondary treatment (i.e. high-rate anaerobic digestion followed by activated sludge digestion). Representative characteristics of this wastewater are shown in Table 1. It should be noted

Table 1 Characteristics of the yeast fermentation wastewater used in this study

Characteristic	Value
COD (mg O_2 L^{-1})	3,950
TC (mg L^{-1})	2,020
Total alkalinity (mg L^{-1} as $CaCO_3$)	1,980
TDS (mg L^{-1})	6,300
Conductivity (mS cm^{-1})	10.4
pH	7.8
Redox potential (mV)	−70
Temperature (°C)	30
[Al] before EC (mg L^{-1})	0.41
[Fe] before EC (mg L^{-1})	26.5
[Cl] (mg L^{-1})	2,460

that fermentation wastewater from yeast production is quite similar to that from fuel-ethanol distilleries, although it is typically more dilute due to the large volume of wash water used in the yeast processing [21].

2.2 Voltammetry

Potentiodynamic cyclic voltammetry was conducted using a calibrated (ASTM G5-94) glass polarisation cell (Princeton Applied Research, New Jersey, USA), fitted with graphite counter electrodes and a saturated calomel reference electrode. Samples cut from the electrode sheets were mounted in a flat specimen holder (Princeton Applied Research, New Jersey, USA). The surfaces of all working electrodes were polished according to ASTM G5-94 unless otherwise stated. To minimise fouling, solids were removed from the wastewater by gravity settling for at least 24 h prior to use in the polarisation cell which was maintained using a water bath at 30 ± 1 °C to emulate the outlet temperature of the aerobic digestion stage in the yeast production plant. High purity nitrogen was used for deaeration, while ambient air was used for aerating the cell, the gas flow being 150 cm^3 min^{-1} in either case. Internal resistance (IR drop) within the cell was compensated for automatically by the Radiometer Analytical Voltalab 50 potentiostat.

2.3 Determination of current efficiency

Total metal consumption was investigated in the glass polarisation cell using single-sided plate electrodes, each having an area of 0.004 m^2 and spaced 0.01 m apart. Direct current was supplied galvanostatically. To eliminate sampling error, the entire electrolyte volume was acidified and microwave-digested prior to atomic absorption spectroscopy (AAS) determination of the metal composition. Scoping experiments were first conducted to determine the run time required for 90% decolourisation of fermentation wastewater. This run time (260 min) was subsequently used for all metal consumption tests.

2.4 Analytical procedures

For colour and COD analyses, samples were centrifuged at 11,000 rpm for 5 min to separate out the solid content. Supernatant colour (measured as UV_{475}) was determined using a UV–vis spectrophotometer while COD was measured by the closed-reflux colourimetric method. Reactor pH, temperature and voltage were monitored online while conductivity was measured offline. Nitric acid digestion of organics, trace metal and chloride analysis, solids analysis, Total Carbon (TC), COD and alkalinity were measured according to APHA/AWWA Standard Methods (21st Edition, 2005).

3 Results and discussion

3.1 Cyclic voltammetry

The behaviour of both electrode materials (i.e. steel and aluminium) in fermentation wastewater were examined across a wide potential range, encompassing the practical operating range for EC with fermentation wastewater, corresponding to j = 1–5 mA cm^{-2}.

The HRC steel data are shown in Fig. 1. At point 1, the steel has an unpolarised potential of $E_{corr} = -0.43$ V. The anodic scan showed very little current until pitting was initiated at approximately $E_{pit} = -0.16$ V (point 2). The reverse scan (from point 3 to 4) recorded a higher current than the forward scan (from point 2 to 3) due to the establishment of localised pits on the anode surface. These pits behave in a similar fashion to those formed by the galvanic pitting corrosion of an unpolarised metal surface; inside the pits, the generation of metal cations attracts anions (particularly Cl^-) while metal hydrolysis lowers the pH. This leads to an aggressive corrosion environment, thus propagating the pits and increasing voltage efficiency. There was no evidence of anodic protection on the reverse scan. The cathodic reduction curve exhibited a potential arrest between points 5 and 6, which is characteristic of a dual passive film being reduced, composed of an inner layer of Fe_3O_4 and an outer layer of γ-Fe_2O_3 [20, 22]. This potential arrest indicated that the reduction of the outer layer is activation limited approaching a current density of 0.01 mA cm^{-2}. The reverse scan (from point 7 to 8) followed the forward scan above j = 0.1 mA cm^{-2}, before repassivating at $E_{pro} = -0.93$ V.

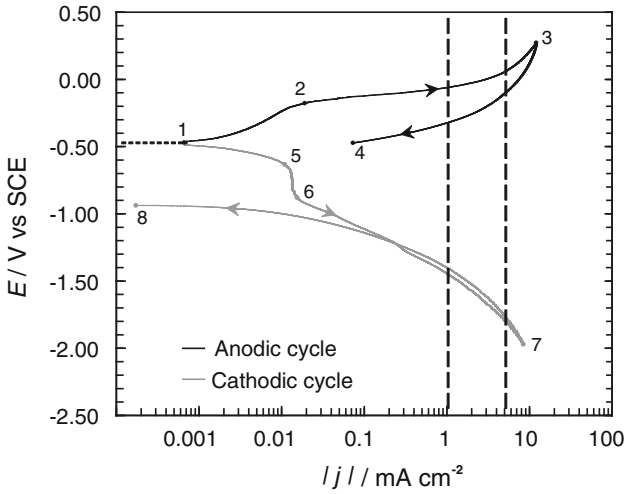

Fig. 1 Cyclic voltammogram for HRC steel in aerated fermentation wastewater. Scan rate = 0.5 mV s^{-1}

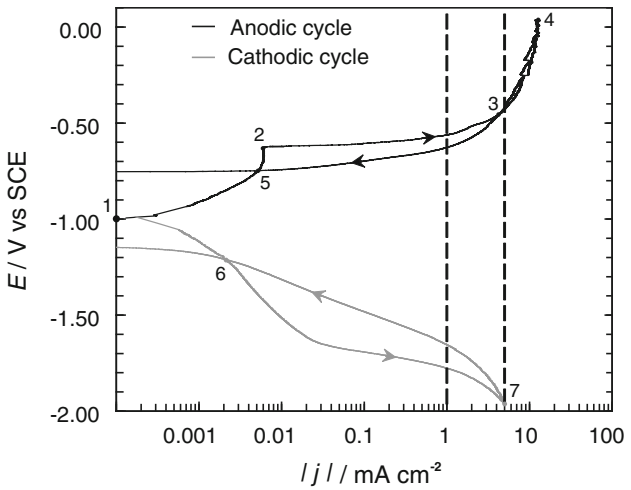

Fig. 2 Cyclic voltammogram for 5005 aluminium in aerated fermentation wastewater. Hysteresis loops are observed on the anodic cycle (point 2 → 3 → 5) and cathodic cycle (point 6 → 7 → 6). Scan rate = 0.5 mV s^{-1}

Aluminium cyclic voltammetry displayed quite different corrosion characteristics to steel (as shown in Fig. 2). The anodic cycle and cathodic cycles both exhibit hysteresis loops and surface protection (i.e. repassivation) on the reverse scan, while the anode exhibited a very pronounced pitting breakthrough (point 2). The closing of the anodic loop above approximately $E_{app} = -0.46$ V (between point 3 and 4) shows that the surface morphology is rapidly established, whereas for HRC steel the pits continue to grow throughout the scan period. The tendency for aluminium to repassivate is a desirable attribute for an EC process because the electrodes will resist corrosion when the reactor is idle, thereby minimising unwanted metal loss. By comparison, steel anodes do not exhibit such self-protection and will continue to corrode at a low rate even when the reactor is not in operation.

Comparing the two anodic pitting hysteresis loops, the required potential for aluminium was not significantly affected over the practical current density range of 1–5 mA cm^{-2}. However, steel has a large potential difference between the forward and reverse scans, demonstrating the influence of pitting corrosion on the power requirement for an operational EC process.

The relationship between current density and potential is essentially linear for both electrode materials over the practical current density operating range. This feature is important in that it indicates that the dominant electrode reactions here are mass transfer (rather than charge transfer) controlled.

3.2 Surface morphology

Corrosion behaviour was also analysed by examining (light microscope) micrographs of the electrode surfaces after each polarisation cycle (Fig. 3). The pitting character of the anodes was found to correlate well with the voltammetry data, as steel exhibited large, irregular pits whereas aluminium exhibited more evenly distributed corrosion. From an operational EC reactor perspective, the irregular pitting of HRC steel would adversely affect electrode life through premature perforation which would both weaken the electrode and give rise to non-uniform coagulant generation within the reactor.

Anodic brightening of the pits is apparent in Fig. 3c, which is characteristic of a thin oxide film [23] contaminated by adsorbed chloride. The high chloride content of fermentation wastewater also accounts for the absence of aluminium passivation under these experimental conditions. Jiang [24] observed the depassivating effect of chloride on aluminium during EC and proposed that chloride 'contaminates' the surface oxide layer, causing strong localised electric field variations in the film, which in turn allows cations to egress. Comparing Fig. 3a and c, it is clear that anodic corrosion of aluminium is more evenly distributed than for HRC steel. From an operational perspective, the absence of passivation removes the need for depassivation measures such as polarity switching or mechanical/chemical cleaning. Thus a high chloride concentration is a desirable characteristic for aluminium electrodes, but detrimental for HRC steel electrodes (by causing uneven pitting corrosion).

In order to accurately determine actual metal consumption in the EC process, metal yields must be measured directly, as discussed next.

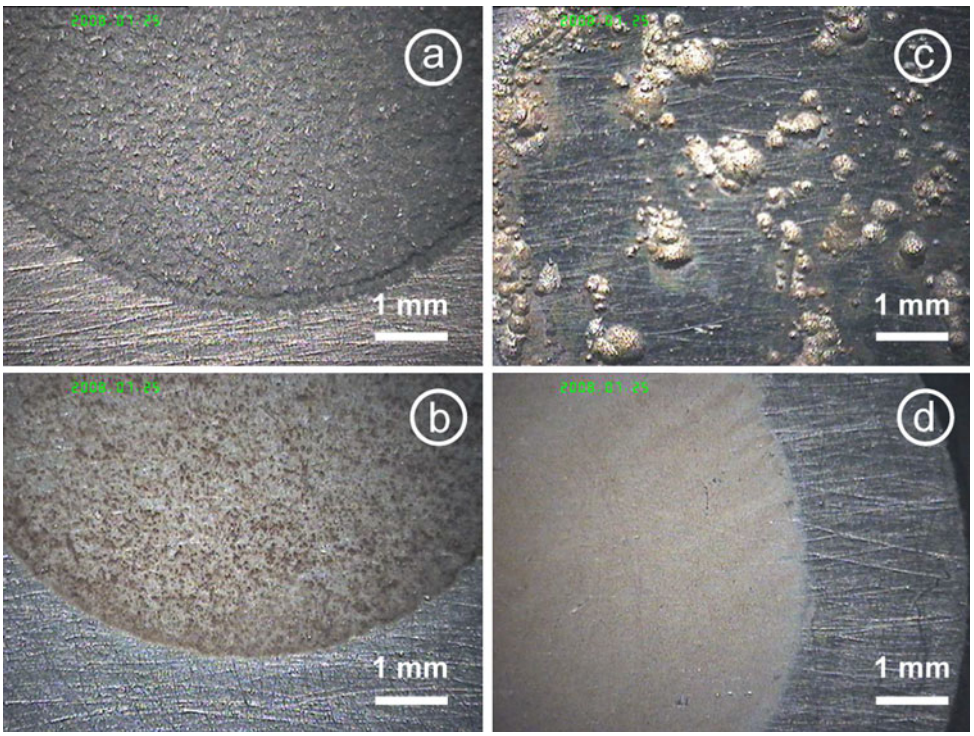

Fig. 3 Micrographs of electrode surfaces after cyclic voltammetry: **a** Al anode, **b** Al cathode, **c** Fe anode and **d** Fe cathode. Note that *brown* discolouration on the Al cathode is caused by melanoidin staining

3.3 Current efficiencies

The concentration of metal was measured by AAS of the electrolyte from the polarisation cell using three different electrode combinations. For comparison, two electrolytes were used—the fermentation wastewater and a NaCl solution of the same conductivity ($\sigma = 10.4$ mS cm^{-1}; [NaCl] = 75 mM). From the measured metal concentrations, current efficiencies were calculated assuming either Fe^{2+} or Al^{3+} corrosion (Fig. 4).

The extent to which cathodic corrosion contributes to overall aluminium consumption is a critical factor in the feasibility of large-scale EC treatment, as metal consumption is the dominant operating cost component. The cathodic corrosion is visible in Fig. 3b and is also evident from the cathodic hysteresis loop formed between points 5 and 6 in the aluminium voltammogram (Fig. 2). Such corrosion is caused by a chemical reaction involving hydroxide ions [13]:

$$2Al_{(s)} + 6H_2O + 2OH^- \rightarrow 2Al(OH)_4^- + 3H_{2(g)} \quad (6)$$

The electrochemical generation of hydroxyl ions from the decomposition of water at the cathode surface (Eq. 2) drives this reaction. To determine the relative contribution of chemical cathodic dissolution to the overall aluminium yield, two polished electrode combinations were tested. One employed two aluminium electrodes, while the other utilised an aluminium anode with a 316 stainless steel (SS) cathode. From the results in Fig. 4 below, it is apparent that

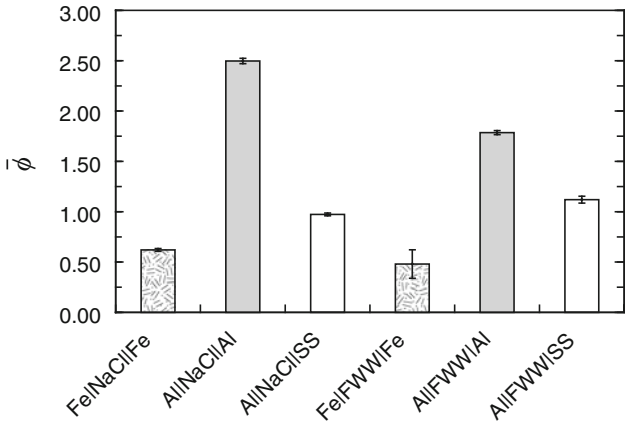

Fig. 4 Mean current efficiency for polished electrode combinations using a pre-aerated electrolyte (NaCl solution or fermentation wastewater; j = 2.5 mA cm^{-2}. Aluminium data published in [26])

anomalous anodic dissolution is present but as a minor contributor to ϕ, on the other hand cathodic corrosion contributes a relatively large proportion of the ϕ. The anomalous anodic dissolution in fermentation wastewater is possibly due to 'chunking', univalent (Al^+) corrosion or chemical corrosion of the anode [14, 15, 25].

The mean current efficiency for steel electrodes was 62% in NaCl solution but somewhat lower ($\bar{\phi} = 48\%$) for fermentation wastewater. These results are consistent with the (relatively slow) establishment of an iron hydroxide layer on the polished anode surface [18, 27]. To test this hypothesis, steel plates were operated at the experimental

current density (j = 2.5 mA cm^{-2}) for 7 h in fermentation wastewater to allow the full development of the surface morphology, thus 'aging' the plates and providing a more accurate measure of steady state behaviour. Immediately after aging, the current efficiency experiment was repeated in fresh wastewater, yielding $\bar{\phi} = 69\%$ (triplicate mean). This increase in $\bar{\phi}$ confirms that a transient aging process of the electrodes results in a considerable reduction of metal yield. Assuming the overall electrochemical reaction was ferric, the current efficiency approached faradaic unity ($\bar{\phi} = 104\%$), raising the possibility that ferric corrosion is the dominant half-cell reaction in this system.

The relationship between current density and current efficiency was investigated for the three electrode combinations (Fig. 5). For steel, there is a downward trend in the current efficiency with increasing current density, while for aluminium the trend is reversed. The downward trend in current efficiency for steel may be associated with the development of a transient surface layer as previously identified. The measured variability in current efficiency highlights the importance of nonfaradaic processes in an operational EC reactor, both in terms of controlling the metal dosage rate and in its implications for plate-life and overall process economics.

3.4 Iron(II) and iron(III) under aerated and deaerated conditions

The issue as to whether iron goes into solution as ferrous or ferric ions, and the fate of the iron species in solution, are matters of considerable concern for an operational EC reactor employing steel electrodes. For example, melanoidins can act as reductants, transforming ferric iron to ferrous iron in the bulk solution. This chemical redox reaction process will not affect the operational Y_{Fe}, however this does affect coagulation performance as ferric coagulants destabilise the negatively charged melanoidins more effectively than ferrous coagulants (Schulze–Hardy rule). Control of the iron oxidation state in the bulk solution can be achieved by gas sparging with nitrogen (stripping out dissolved oxygen and thus favouring ferrous speciation) or air/oxygen (increasing the dissolved oxygen concentration and thus favouring ferric speciation). The use of gas sparging in an operational EC process would augment the flotation separation provided by cathodic gas generation.

Results are presented in Table 2 and Fig. 6 from the polarisation cell treating fermentation wastewater where nitrogen or air sparging was employed. Aerated fermentation wastewater decolourised at approximately twice the rate of deaerated effluent. During treatment, the observed colour of the two suspensions differed markedly. Red rust was observed in the aerated case (indicating ferric speciation) while green rust was observed in the deaerated case (indicating ferrous speciation). After 19.5 h of operation, the metal concentration was measured with the calculated ferric current efficiency being 98.4% for the aerated conditions and 100% for the deaerated case.

Table 2 Wastewater characteristics and current efficiencies under aerated and deaerated conditions

	Aerated	Deaerated
Initial redox potential	−0.057 V	−0.113 V
Final pH	8.6	9.2
Current efficiency (Fe^{2+}) (%)	65.6	66.7
Current efficiency (Fe^{3+}) (%)	98.4	100.0
Time required for $UV_t/UV_0 < 0.10$ (h)	7.6	15.0
Observed colour	Reddish-brown	Green

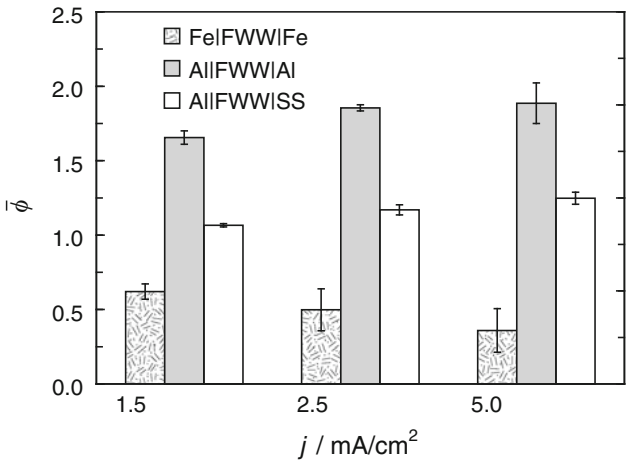

Fig. 5 Mean current efficiency at different current densities for polished electrode combinations in pre-aerated fermentation wastewater

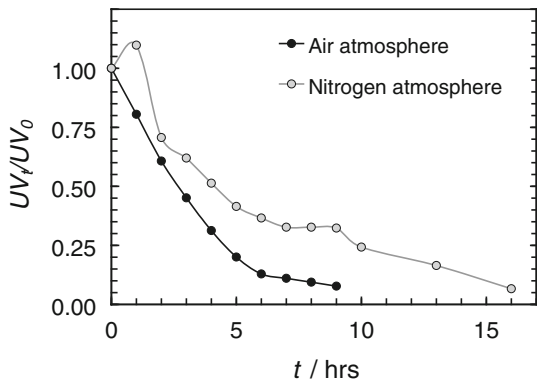

Fig. 6 Decolourisation profile for EC of fermentation wastewater using HRC steel electrodes (aged for 7 h) under aerated and deaerated conditions

These results demonstrate that bulk redox potential has a strong influence on iron speciation and coagulation performance within the bulk solution of an operational EC reactor, but has negligible impact on the corrosion rate at the electrode interface. The current efficiency data again approach faradaic unity for ferric corrosion, the exact mechanism for this process requires further investigation. These results also indicate that reactor aeration by Dissolved Air Flotation (DAF) is an attractive option to consider with EC. The bubbles generated by DAF are very small (typically 40 μm mean diameter) thereby maximising oxygen transfer to favour ferric speciation and intensifying the solids removal rate by flotation.

4 Conclusions

Remediation of biologically treated wastewater from molasses-fed fermentation is a significant technical challenge due to the high loadings of biorecalcitrant melanoidins. Electrocoagulation (EC) is an alternative coagulation technology that is capable of removing 99% of the colour and 80% of the COD from this wastewater. For operational and economic reasons, the corrosion behaviour of steel and aluminium electrodes is a critical consideration for EC, and one that has not been previously explored in detail for fermentation wastewater. The discussion presented here provides practical insights into the underlying corrosion characteristics which assist in electrode selection and EC reactor optimisation. Summarising the findings for EC using 5005 aluminium electrodes:

- Chemical corrosion of the cathode contributes a significant fraction of the overall metal yield;
- Anomalous anodic corrosion also contributes to overall metal consumption;
- Chloride (typically 2.6 g L^{-1} in fermentation wastewater) acts as an effective depassivating agent over a wide potential range.

and for EC utilising HRC steel electrodes:

- Heavy, irregular pitting of the anode would be expected to cause both current density variations and premature perforation of the electrode;
- Current efficiency data revealed a Fe^{3+} current efficiency of $\sim$100% when aged plates were employed, raising the possibility that ferric corrosion is the dominant electrochemical reaction at the anode;
- Formation of a dual layer surface oxide on the polished anode caused a transient current efficiency loss that is larger at higher current density;
- Aeration of an EC reactor maximises ferric speciation in the bulk solution and augments solid separation by flotation, without affecting current efficiency.

Ongoing research is focussed on the influence of bulk solution pH on coagulation performance, the mechanism of ferric corrosion, and the role that (polymeric) flocculation aids and DAF can play in improving solid separation and dewatering.

Acknowledgements This work was funded by the Australian Research Council Linkage Project LP0669783 in conjunction with AB Mauri Ltd.

References

1. Chen G (2004) Sep Purif Technol 11:38
2. Juttner K, Galla U, Schmieder H (2000) Electrochim Acta 2575:45
3. Tewari P, Batra V, Balakrishnan M (2007) Resour Conserv Recycl 351:52
4. Dwyer J, Kavanagh L, Lant P (2008) Chemosphere 1745:71
5. Alfafara C, Migo V, Amarante J et al (2000) Water Sci Technol 193:42
6. Satyawali Y, Balakrishnan M (2008) J Environ Manag 481:86
7. Mickley M (2003) Membr Technol 8
8. Pandey R, Malhotra S, Tankhiwale A et al (2003) Int J Environ Stud 263:60
9. Mollah M, Schennach R, Parga J et al (2001) J Hazard Mater 29:84
10. Ryan D, Gadd A, Kavanagh J et al (2008) Sep Purif Technol 347:58
11. Linares-Hernandez I, Barrera-Diaz C, Roa-Morales G et al (2007) J Hazard Mater 240:144
12. Van de Ven E, Koelmans H (1976) J Electrochem Soc 143:123
13. Moon S, Pyun S (1997) Corros Sci 399:39
14. Garreau M, Bonora P (1977) J Appl Electrochem 197:7
15. Vautrin-Ul C, Taleb A, Stafiej J et al (2007) Electrochim Acta 7802:52
16. Lakshmanan D, Clifford D, Samanta G (2009) Environ Sci Technol 3853:43
17. Mileham A, Jones R, Harvey S (1982) Precis Eng 168:4
18. Shao H, Wang J, He W et al (2005) Electrochem Commun 1429:7
19. Alsheyab M, Jiang J, Stanford C (2009) J Environ Manag 1350:90
20. De Koninck M, Brousse T, Belanger D (2003) Electrochim Acta 1425:48
21. Kobya M, Delipinar S (2007) J Hazard Mater 1133:154
22. Rauscher A, Konno H, Nagayama M (1977) Electrochim Acta 823:22
23. Hoar T, Mears D, Rothwell G (1965) Corros Sci 279:5
24. Jiang J (1988) Water Treat 344:3
25. Gu Z, Liao Z, Schulz M et al (2009) Ind Eng Chem Res 3112:48
26. Gadd A, Ryan D, Kavanagh J et al (2010) Water Sci Technol (in press, accepted manuscript)
27. Den W, Huang C, Ke H (2006) A mechanistic study on the electrocoagulation of silica nanoparticles from polishing wastewater. In: Water practice & technology. IWA Publishing. www.iwaponline.com/wpt/001/wpt0010049.htm. Cited 19 January 2010